A Quadratic-Interpolated LUT-Based Digital Predistortion Technique for Cellular Power Amplifiers

Ken-Fu Liang, Jau-Horng Chen, *Member, IEEE*, and Yi-Jan Emery Chen, *Senior Member, IEEE*

***Abstract*—Baseband digital predistortion (DPD) is an efficient and low-cost method for linearizing a power amplifier (PA) in a wireless system using a modulation scheme with nonconstant envelope. The polynomial and the lookup table (LUT) predistortion schemes are two commonly used approaches. Both approaches require time to find the inverse characteristics of the PA to be predistorted. However, for DPD to be actually implemented in real-world scenarios, fast convergence is highly desirable. A low-complexity joint-polynomial/LUT predistortion PA linearizer is proposed to obtain fast linearization. The algorithm utilizes quadratic interpolation of the LUT, which reduces the required LUT size and hence reduces convergence time without degradation of linearity. Simulation result shows that the proposed method can achieve up to 500% improvement in convergence speed compared with the conventional linear interpolation approach for the wideband code-division multiple access application.**

***Index Terms*—Digital predistortion (DPD), linearization, lookup table (LUT), power amplifier (PA).**

I. Introduction

With the widespread use of wireless communication systems, modern communication standards utilize highly complex modulation schemes to increase spectral efficiency. These complex modulation schemes often have nonconstant envelopes that are required to be amplified linearly. Moreover, these modulation schemes often possess very high peak-to-average power ratios (PAPR) and necessitate the power amplifier (PA) to be backed off accordingly, which leads to low PA power efficiency. Various linearization methods have been proposed in [1]–[13] to improve PA efficiency, whereas digital predistortion (DPD) is one of the most widely used techniques, particularly in base stations and mobile systems.

The polynomial and the lookup table (LUT) are two of the most widely used methods for implementing DPD systems. In this brief, a joint-polynomial/LUT method is proposed to improve the convergence time of the DPD systems. The proposed method requires less LUT entries such that it will take less time to populate them and hence lead to shorter convergence time. The fast convergence characteristic is highly attractive for mobile systems in which the ambient environment is always changing and dynamic power control is utilized.

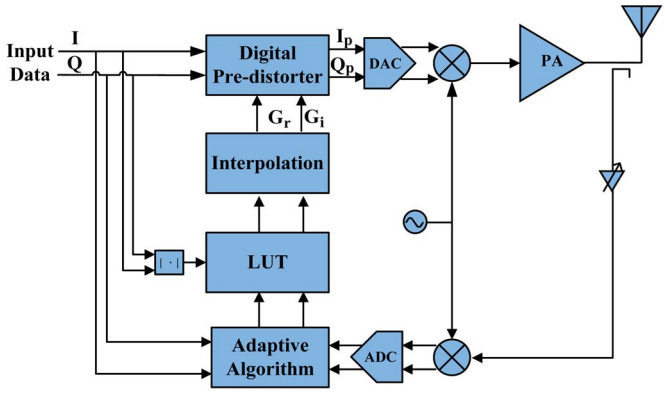

Fig. 1. Block diagram of an adaptive DPD system.

II. System Model and Predistortion

The PA's nonlinear characteristics consist of a static part and a dynamic part. The static part includes the amplitude-dependent gain and phase shifts, or AM–AM and AM–PM conversion functions, respectively. The gain function can be written as

$$G(r) = K(r) \cdot e^{\phi(r)} \tag{1}$$

where r is the input amplitude, $K(\cdot)$ is the AM–AM function, and $\phi(\cdot)$ is the AM–PM function. The dynamic part consists of the memory effect, which causes the output signal to be dependent on not only the current input signal but also the input signal at a prior state. In this brief, the handset PAs with low memory effects are considered as in [14] and [15]. The block diagram of an adaptive DPD system is shown in Fig. 1. The primary functionality is usually realized in digital logic, with a predistortion block operating on the modulated digital baseband signal prior to digital-to-analog conversion and frequency up-conversion. The predistortion block would predistort the input signal by using the LUT values with interpolation. Assuming

Manuscript received June 18, 2013; revised September 20, 2013; accepted December 18, 2013. Date of publication January 24, 2014; date of current version March 14, 2014. This work was supported in part by the National Science Council of Taiwan under Grants NSC 100-2221-E-002-092-MY3, 100-2221-E-002-093-MY3, 100-2221-E-002-094-MY3, and 102-2218-E-002-005. This brief was recommended by Associate Editor T. Li.

K.-F. Liang and Y.-J. E. Chen are with the Department of Electrical Engineering, Graduate Institute of Communication Engineering, and Graduate Institute of Electronics Engineering, National Taiwan University, Taipei 106, Taiwan (e-mail: emery@cc.ee.ntu.edu.tw).

J.-H. Chen is with the Department of Engineering Science and Ocean Engineering, National Taiwan University, Taipei 106, Taiwan (e-mail: jauchen@ntu.edu.tw).

Color versions of one or more of the figures in this brief are available online at http://ieeexplore.ieee.org.

Digital Object Identifier 10.1109/TCSII.2013.2296194

the input of the predistorter is a modulated complex baseband signal as

$$V_m = I + jQ. \tag{2}$$

The output signal of the predistortion block can be written as

$$V_d = I_p + jQ_p = V_m \cdot F\left(|V_m|\right) \tag{3}$$

where the characteristic of the predistorter is denoted by $F(\cdot)$. V_d, V_m, and $F(|V_m|)$ are all in complex form. When predistortion is utilized, the output signal of the PA can then be modeled as

$$V_a = V_d \cdot G\left(|V_d|\right) \tag{4}$$

where V_a, V_d, and $G(|V_d|)$ are all in complex form, and $G(\cdot)$ consists of the AM–AM and AM–PM effects of the PA, whereas the carrier frequency component is neglected for simplicity as in [11]. Overall, the output signal of a predistorted PA can be rewritten as

$$V_a = V_m \cdot F\left(|V_m|\right) \cdot G\left(|V_m \cdot F\left(|V_m|\right)|\right). \tag{5}$$

If DPD is used to cancel the AM–AM and AM–PM nonidealities, an overall linear PA system with constant gain can be obtained. The overall output signal can be written as

$$V_a = A \cdot V_m \tag{6}$$

where A is the constant overall signal gain.

A variety of DPD techniques have been previously developed [8]–[11]. A complex-gain LUT approach [9] is chosen for this implementation to enable the DPD system to be quickly converged for adaptation. Additionally, IQ magnitude is chosen for LUT addressing, as shown in [8], to optimize the dynamic range of correction with a minimal number of LUT entries for fast adaptation at the start of transmission.

The LUTs of the LUT-based DPD systems can be implemented in Cartesian form [1], polar form [2], and complex-gain form [9]. No matter how the LUTs are implemented, to populate an LUT properly such that the LUT can represent the inverse function of the PA is the most important task in implementing an LUT-based linearizer. This study focuses on a complex-gain LUT-based predistorter configuration, in which the real and imaginary parts of the predistorter mapping function are quantized rather than the magnitude and phase.

When implementing an LUT-based DPD system, using input–output comparison to directly update the LUT entries is the simplest method. The LUT entry can be updated by

$$F_{k+1}^{[n]} = F_k^{[n]} + \alpha \cdot e_k \tag{7}$$

where α is the step size, and $F_k^{[n]}$ and $F_{k+1}^{[n]}$ are the nth LUT values at time k and $k+1$, respectively. e_k is the error vector at time k defined as

$$e_k = V_m - V_a. \tag{8}$$

The least mean square (LMS) algorithm [16] is a widely used algorithm to increase the convergence speed of LUTs. The LMS algorithm is chosen because of its low complexity and high stability. The LMS algorithm updates the LUT with

$$F_{k+1}^{[n]} = F_k^{[n]} + \alpha \cdot \left(V_m^*\right)\left(e_k\right) \tag{9}$$

where V_m^* is the conjugate of the input sample. The parameter $\alpha = 7/32$ is used in the simulation. Once the LUT has converged, the RF feedback path and LUT update logic can be powered down to reduce power dissipation.

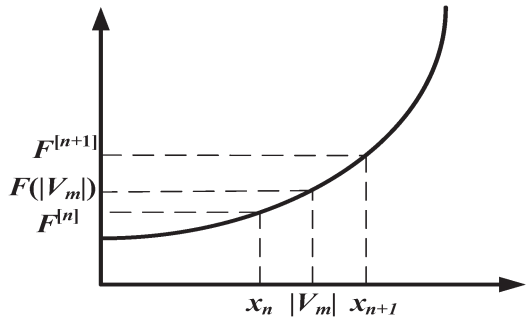

Fig. 2. Example of an interpolated LUT entry.

III. Quadratic–Interpolated LUT Method

In an LUT-based predistorter, each LUT entry describes only one single point of the inverse PA characteristics. To have a better approximation of the inverse of the PA's nonlinear characteristics, one method is to increase the number of LUT entries such that quantization error is reduced, as shown in [17]. However, an increased number of LUT entries leads to a longer convergence time, and its implementation requires more logic gates. Another method is to use linear–interpolated LUTs, which have been experimentally shown to improve performance in [2], [12], and [13]. The linear–interpolated LUT method uses linear interpolation between adjacent LUT entries for both predistortion and LUT updates. Because the input value $|V_m|$ will not always be located on the LUT index, using interpolation between the adjacent LUT indices (the nth and $n+1$th) will reduce the quantization error. Fig. 2 shows an example of an interpolated LUT entry. In the case of linear interpolation, the interpolated LUT entry value can be calculated using

$$F\left(|V_m|\right) = F_k^{[n]} + \frac{F_k^{[n+1]} - F_k^{[n]}}{T_{\text{res}}}\left(|V_m| - x_n\right) \tag{10}$$

where $F_k^{[n]}$ and $F_k^{[n+1]}$ are the nth and $n+1$th LUT values at time k, respectively. x_n is the corresponding voltage of the nth LUT index, and T_{res} is the resolution of LUT indices and is defined as

$$T_{\text{res}} = \frac{R}{N} \tag{11}$$

where R is the range of the input value $|V_m|$ and N is the number of the LUT entries, which can be chosen as the order of 2 and implemented in hardware by a logic shifter.

Linear interpolation with adjacent LUT entries provides first-order approximation for input values between indices. An

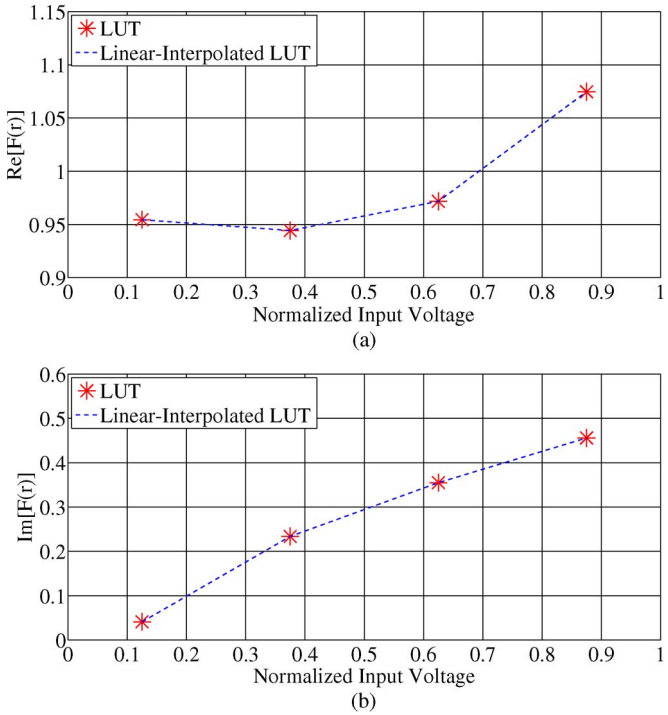

Fig. 3. Linear interpolation of a complex gain. (a) Re$[F(\cdot)]$. (b) Im$[F(\cdot)]$.

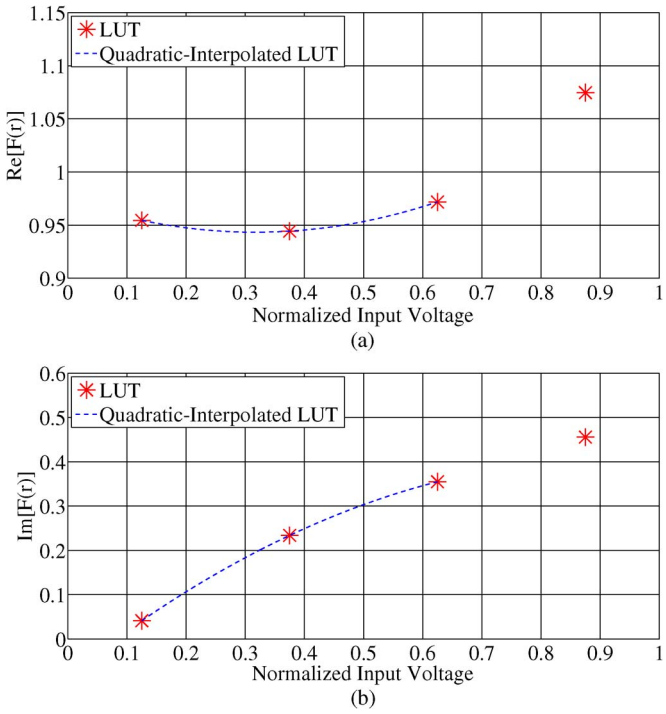

Fig. 4. Quadratic interpolation of a complex gain. (a) Re$[F(\cdot)]$. (b) Im$[F(\cdot)]$.

example of the complex-gain linear–interpolated LUT method is shown in Fig. 3. Compared with a noninterpolated LUT, a linear–interpolated LUT can model the inverse PA characteristic more accurately. However, there is still room for improvement since the inverse function should be a smooth curve. Therefore, the linear–interpolated LUT method may cause spectrum regrowth and increased noise floor. To further improve the performance of the interpolated-LUT DPD system, another interpolation technique is needed. Various interpolation methods have been proposed in [18] and [19]. Due to the complexity and hardware implementation, a complex-gain quadratic–interpolated LUT-based DPD system is proposed.

The inverse characteristic of a PA can be more accurately modeled with high-order polynomials. However, the complexity of implementation and amount of computation do not justify the high accuracy. Instead of using high-order polynomials for modeling the global inverse PA characteristic, the proposed quadratic–interpolated LUT is used to describe the local inverse PA characteristic while preserving the benefits of an LUT-based DPD system. With computation complexity kept in mind, the quadratic interpolation was chosen over the interpolation with higher order polynomials. When the input voltage $|V_m|$ is closest to the nth LUT index, the $n-1$th, nth, and $n+1$th LUT values are used to calculate the quadratic polynomial function

$$F(|V_m|) = f^{[n-1]}(|V_m|) \cdot F_k^{[n-1]} + f^{[n]}(|V_m|) \cdot F_k^{[n]} + f^{[n+1]}(|V_m|) \cdot F_k^{[n+1]} \quad (12)$$

where $F_k^{[n-1]}$, $F_k^{[n]}$ and $F_k^{[n+1]}$ are the n-1th, nth, and $n+1$th LUT values at time k, respectively. $f^{[n-1]}(\cdot)$, $f^{[n]}(\cdot)$, and $f^{[n+1]}(\cdot)$ are the weighting functions that can be calculated as

$$f^{[n-1]}(|V_m|) = \frac{(|V_m| - x_n)(|V_m| - x_{n+1})}{(x_{n-1} - x_n)(x_{n-1} - x_{n+1})} \quad (13)$$

$$f^{[n]}(|V_m|) = \frac{(|V_m| - x_{n-1})(|V_m| - x_{n+1})}{(x_n - x_{n-1})(x_n - x_{n+1})} \quad (14)$$

$$f^{[n+1]}(|V_m|) = \frac{(|V_m| - x_{n-1})(|V_m| - x_n)}{(x_{n+1} - x_{n-1})(x_{n+1} - x_n)} \quad (15)$$

where x_{n-1} and x_{n+1} are corresponding voltage of $n-1$th and $n+1$th LUT indices, respectively. If the LUT is indexed with uniform spacing, the equations can be rewritten as

$$f^{[n-1]}(|V_m|) = \frac{(|V_m| - x_n)(|V_m| - x_{n+1})}{2T_{\text{res}}^2} \quad (16)$$

$$f^{[n]}(|V_m|) = \frac{(|V_m| - x_{n-1})(|V_m| - x_{n+1})}{T_{\text{res}}^2} \quad (17)$$

$$f^{[n+1]}(|V_m|) = \frac{(|V_m| - x_{n-1})(|V_m| - x_n)}{2T_{\text{res}}^2} \quad (18)$$

where T_{res} is the resolution of LUT indices. An example of the quadratic–interpolated LUT method is shown in Fig. 4. It can be seen that the use of quadratic interpolation leads to continuous slope at the LUT indices, which will result in better spectral output results compared with the noninterpolated or the linear–interpolated LUT approach. By choosing T_{res} to be the order of 2, the divisions can be achieved with logic shifters. As a result, the proposed method will have similar computation complexity to that of the linear–interpolated LUT method.

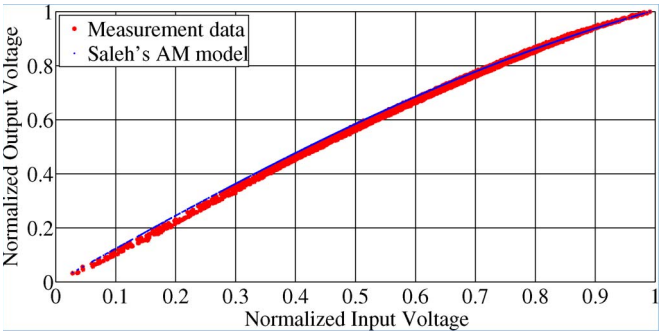

Fig. 5. AM–AM of Saleh's model and real PA.

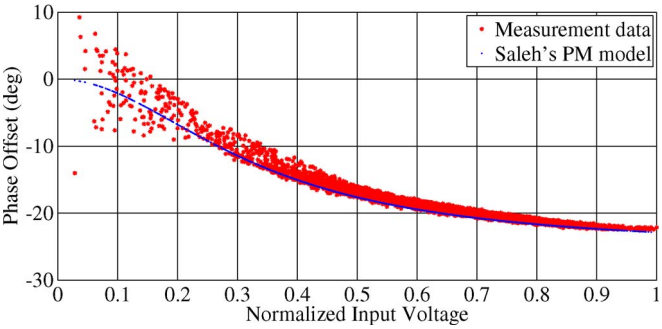

Fig. 6. AM–PM of Saleh's model and real PA.

IV. Simulation Results

The proposed algorithm has been tested with MATLAB, using Saleh's PA model in [20] exhibiting AM–AM and AM–PM characteristics. The AM–AM and AM–PM properties of the PA with input amplitude r can be expressed as

$$K(r) = \frac{\alpha_a r}{1 + \beta_a r^2} \tag{19}$$

$$\Phi(r) = \frac{\alpha_p r^2}{1 + \beta_p r^2} \tag{20}$$

where $K(r)$ and $\Phi(r)$ are the amplitude and the phase responses of the PA's nonlinear characteristics, respectively. The parameters $\alpha_a = 2.2$, $\beta_a = 0.23$, $\alpha_p = -4.033$, and $\beta_p = 9.104$ were chosen in our initial simulation, which correspond to a real PA used with negligible memory effects. The PA model is shown in Figs. 5 and 6. The normalized input is in the range of 0–1, and the model leads to a maximum gain compression of 6.56 dB and phase deviation of $-22.87°$.

The simulations were performed in the baseband domain using a wideband code-division multiple access (WCDMA) voice signal. Fig. 7 shows the simulated output spectrums of the linearly amplified input signal, together with the PA output signal under various conditions of interest. Spectral regrowth characteristics were evident because of the PA's nonlinear characteristics. The proposed four-entry quadratic–interpolated LUT achieves more linearity improvement than a conventional four-entry linear–interpolated LUT. To compare the accuracy of the proposed and conventional LUT-based DPD systems, simulations were performed with both four and eight LUT entries. The averaged adjacent channel leakage ratio (ACLR) is summarized in Table I. ACLR is defined as the ratio of the power in the adjacent or alternate channel to the transmitted power. By using the same number of LUT entries, the quadratic–interpolated LUT had better ACLR than the linear–interpolated LUT. It can be seen that using a quadratic–interpolated LUT with four entries had similar results to those of a linear–interpolated LUT with eight entries. Usually, an LUT with fewer entries will take less time to converge. To assess the convergence speed, transient ACLR simulations were performed. Due to a large amount of data, results were recorded every 100 iterations. The simulation results are shown in Fig. 8. The transient ACLR is a clear index that the proposed quadratic LUT method converges much more quickly than the conventional method because fewer LUT entries are needed. The quadratic–interpolated LUT takes about 950 iteration times to reach an ACLR of -53 dB, whereas the linear–interpolated LUT takes about 4750 iteration times.

To further assess the performance of the proposed method, simulations were carried out using a Long-Term Evolution (LTE) signal, which has higher PAPR compared with a WCDMA voice signal. Fig. 9 shows the simulated output spectrums under various conditions with four LUT entries.

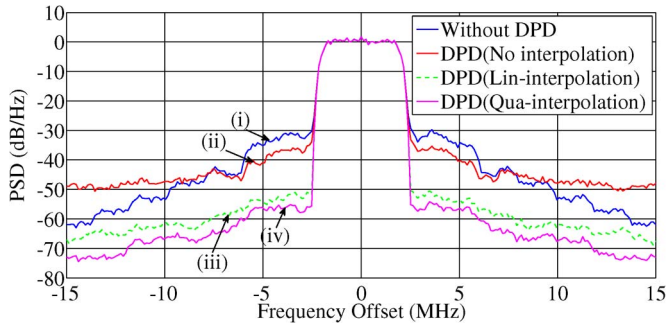

Fig. 7. Simulated WCDMA signal spectrum before and after linearization. (i) Without linearization, (ii) predistortion without interpolation, (iii) predistortion with linear interpolation, and (iv) predistortion with quadratic interpolation.

TABLE I
Simulated ACLR of WCDMA Signal With Different LUTs

	4 entries		8 entries	
	ACLR1	ACLR2	ACLR1	ACLR2
Non-interpolated	-38.2 dB	-41.5 dB	-46.9 dB	-48.1 dB
Linear-interpolated	-55.0 dB	-60.0 dB	-61.8 dB	-65.6 dB
Quadratic-interpolated	-58.3 dB	-64.6 dB	-62.1 dB	-66.6 dB

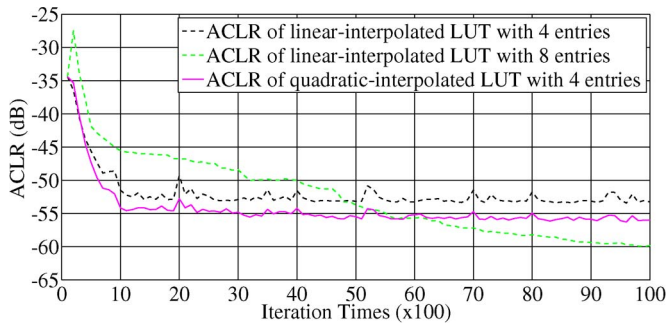

Fig. 8. WCDMA ACLR convergence performance of linear– and quadratic–interpolated LUTs.

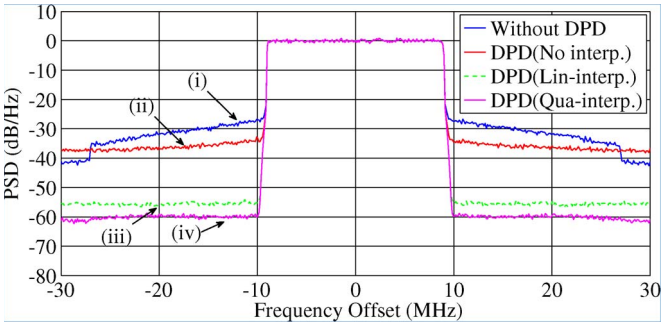

Fig. 9. Simulated LTE signal spectrum before and after linearization. (i) Without linearization, (ii) predistortion without interpolation, (iii) predistortion with linear interpolation, and (iv) predistortion with quadratic interpolation.

TABLE II
SIMULATED ACLR OF THE LTE SIGNAL WITH DIFFERENT LUTS

	4 entries	8 entries
	ACLR1	ACLR1
Non-interpolated	-36.2 dB	-40.4 dB
Linear-interpolated	-55.5 dB	-63.9 dB
Quadratic-interpolated	-60.3 dB	-66.5 dB

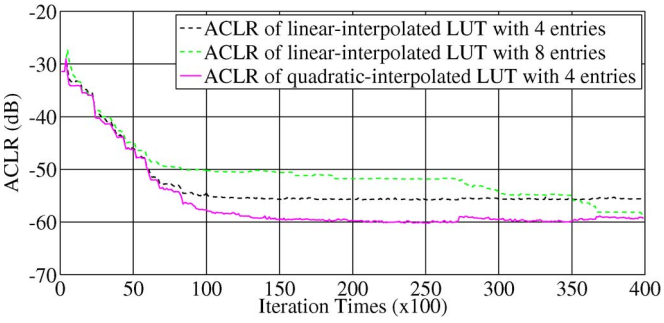

Fig. 10. LTE ACLR convergence performance of linear– and quadratic–interpolated LUTs.

TABLE III
SIMULATED ACLR CONVERGENCE SPEED

	4 entries	8 entries	Improvement
Iteration times at ACLR of -53dB for WCDMA	950	4750	500%
Iteration times at ACLR of -53dB for LTE	6750	27900	413%

The proposed quadratic–interpolated LUT method had the best linearization performance. The averaged ACLR simulation results for both four and eight LUT entries are summarized in Table II. The transient results are shown in Fig. 10. A similar result was observed by using a high-PAPR LTE signal. The conversion speed for transient ACLR simulation result is summarized in Table III. The proposed quadratic–interpolated method can lead to significantly faster convergence time while achieving similar linearity result.

V. CONCLUSION

A quadratic–interpolated LUT-based DPD system is proposed. The method provides better fitting for samples between LUT entries, which makes it possible for using fewer LUT entries in LUT-based DPD systems. With fewer LUT entries, faster convergence is attained while maintaining similar linearity improvement. The proposed method has been verified with both WCDMA and LTE signals, which have low and high PAPRs. For both standards, the proposed method showed significant speed improvement while possessing similar computational complexity compared with the conventional linear–interpolated method.

REFERENCES

[1] Y. Nagata, "Linear amplification technique for digital mobile communications," in *Proc. IEEE 39th Veh. Technol. Conf.*, May 1989, pp. 159–164.
[2] M. Faulkner and M. Johansson, "Adaptive linearization using predistortion—Experimental results," *IEEE Trans. Veh. Technol.*, vol. 43, no. 2, pp. 323–332, May 1994.
[3] A. D. Zhu, P. J. Draxler, J. M. J. Yan, T. J. Brazil, D. F. Kimball, and P. M. Asbeck, "Open-loop digital predistorter for RF power amplifiers using dynamic deviation reduction-based Volterra series," *IEEE Trans. Microw. Theory Tech.*, vol. 56, no. 7, pp. 1524–1534, Jul. 2008.
[4] K. Jangheon, P. Changjoon, M. Junghwan, and K. Bumman, "Analysis of adaptive digital feedback linearization techniques," *IEEE Trans. Circuits Syst. I, Reg. Papers*, vol. 57, no. 2, pp. 345–354, Feb. 2010.
[5] H. H. Boo, S. Chung, and J. L. Dawson, "Digitally assisted feedforward compensation of Cartesian-feedback power-amplifier systems," *IEEE Trans. Circuits Syst. II, Exp. Briefs*, vol. 58, no. 8, pp. 457–461, Aug. 2011.
[6] J. Mehta, V. Zoicas, O. Eliezer, R. B. Staszewski, S. Rezeq, M. Entezari, and P. Balsara, "An efficient linearization scheme for a digital polar EDGE transmitter," *IEEE Trans. Circuits Syst. II, Exp. Briefs*, vol. 57, no. 3, pp. 193–197, Mar. 2010.
[7] N. Naskas and Y. Papananos, "Neural-network-based adaptive baseband predistortion method for RF power amplifiers," *IEEE Trans. Circuits Syst. II, Exp. Briefs*, vol. 51, no. 11, pp. 619–623, Nov. 2004.
[8] K. J. Muhonen, M. Kavehrad, and R. Krishnamoorthy, "Look-up table techniques for adaptive digital predistortion: A development and comparison," *IEEE Trans. Veh. Technol.*, vol. 49, no. 5, pp. 1995–2002, Sep. 2000.
[9] J. K. Cavers, "Amplifier linearization using a digital predistorter with fast adaptation and low memory requirements," *IEEE Trans. Veh. Technol.*, vol. 39, no. 4, pp. 374–382, Nov. 1990.
[10] J. K. Cavers, "Optimum table spacing in predistorting amplifier linearizers," *IEEE Trans. Veh. Technol.*, vol. 48, no. 5, pp. 1699–1705, Sep. 1999.
[11] J. Y. Hassani and M. Kamareei, "Quantization error improvement in a digital predistorter for RF power amplifier linearization," in *Proc. IEEE 54th Veh. Technol. Conf.*, Oct. 2001, pp. 1201–1204.
[12] I. Teikari, J. Vankka, and K. Halonen, "Baseband digital predistorter with quadrature error correction," in *Proc. Norchip Conf.*, Nov. 8–9, 2004, pp. 159–162.
[13] G. Norris, J. Staudinger, J.-H. Chen, C. Rey, P. Pratt, and R. Sherman, "Application of digital adaptive pre-distortion to mobile wireless devices," in *Proc. IEEE RFIC Symp. Dig.*, Jun. 2007, pp. 247–250.
[14] D. Junxiong, P. Gudem, L. E. Larson, D. Kimball, and P. M. Asbeck, "A SiGe PA with dual dynamic bias control and memoryless digital predistortion for WCDMA handset applications," in *Proc. IEEE RFIC Symp. Dig.*, Jun. 2005, pp. 247–250.
[15] P. B. Kenington, *High-Linearity RF Amplifier Design*. Norwood, MA, USA: Artech House, 2000.
[16] S. Haykin, *Adaptive Filter Theory*. Englewood Cliffs, NJ, USA: Prentice-Hall, 2002.
[17] S. Chung, J. W. Holloway, and J. L. Dawson, "Open-loop digital predistortion using Cartesian feedback for adaptive RF power amplifier linearization," in *Proc. IEEE MTT-S Int. Microw. Symp. Dig.*, Jun. 2007, pp. 1449–1452.
[18] R. C. de Lamare and R. Sampaio-Neto, "Adaptive reduced-rank MMSE filtering with interpolated FIR filters and adaptive interpolators," *IEEE Signal Process. Lett.*, vol. 12, no. 3, pp. 177–180, Mar. 2005.
[19] R. C. de Lamare and R. Sampaio-Neto, "Adaptive reduced-rank processing based on joint and iterative interpolation, decimation and filtering," *IEEE Trans. Signal Process.*, vol. 57, no. 7, pp. 2503–2514, Jul. 2009.
[20] A. A. M. Saleh, "Frequency-independent and frequency-dependent nonlinear models of TWT amplifiers," *IEEE Trans. Commun.*, vol. COM-29, no. 11, pp. 1715–1720, Nov. 1981.